IOPscience iopscience.iop.org

Home Search Collections Journals About Contact us My IOPscience

Space charge limited field emission in a plane parallel electrode geometry

This article has been downloaded from IOPscience. Please scroll down to see the full text article.

1973 J. Phys. A: Math. Nucl. Gen. 6 1439

(http://iopscience.iop.org/0301-0015/6/9/019)

View the table of contents for this issue, or go to the journal homepage for more

Download details:
IP Address: 171.66.16.87
The article was downloaded on 02/06/2010 at 04:49

Please note that terms and conditions apply.

J. Phys. A: Math., Nucl. Gen., Vol. 6, September 1973. Printed in Great Britain. © 1973

Space charge limited field emission in a plane parallel electrode geometry

C B Wheeler

Plasma Physics Department, Imperial College, London SW7 2AZ, UK

Received 2 April 1973

Abstract. Poisson's equation in parallel geometry is solved analytically with the inclusion of the electron emission velocity spectrum predicted by quantum mechanics. The mathematical difficulty of classically defining the cathode surface is overcome, to a first approximation, by postulating a virtual cathode situated in front of the real cathode such that the majority of the emitted electrons have penetrated the potential barrier at that position. The treatment is nonrelativistic, assumes that the emission is exclusively by barrier penetration, and is expressed in parameters that enable the results to be applied to most situations of interest. It is shown that the effect of nonzero emission velocity is negligible except for the cases of cathodes of low work function operated at very high current densities. Particular attention is paid to the departure of the experimentally measured current from that predicted by the Fowler–Nordheim theory and the subsequent approach to the Langmuir–Child fully space charge limited current. It is shown that the point of departure can quantitatively be defined in terms of the fully limited current and the bearing of this on the design of field emission electron guns is considered.

1. Introduction

At very large values of field strength it is found experimentally that the field emission current density falls significantly below the value predicted by the Fowler–Nordheim (FN) theory. Two explanations have been offered for this observation, one primarily concerned with field strengths and the other with current densities. Cutler and Nagy (1964) suggested that this departure was due to the presence of a short range image force at the cathode potential barrier that is not included in the FN theory. They provide some quantum-mechanical evidence for an inverse-square factor in the barrier that only becomes significant at very high cathode field strengths. On the other hand Stern *et al* (1929) predicted departures from the then recently formulated FN theory when current densities were great enough for the associated space charge to reduce the field at the cathode below the expected value. Their simple treatment, which was later extended by Barbour *et al* (1953), involved solving Poisson's equation in a plane parallel geometry with the simplifying assumption that the electron emission velocity from the cathode was zero. An analysis carried out in curved geometries would be more applicable to field emission experiments but is beset with difficulties in the two successive integrations of Poisson's equation. However, Norwicki (1967) bypassed this difficulty in a spherical geometry by evaluating inter-electrode potentials entirely in terms of a charge distribution composed of an assumed real space charge and its electrostatic image inside the spherical cathode.

A suitable choice of the parameters occurring in both of these approaches enables them to explain the deviation from the FN theory observed in the extensive experiments of Dyke and Trolan (1953) and it is highly likely that the departure is due to a combination of both effects. However, the influence of finite emission velocities on the space charge distribution has at no time been considered. Even though these velocities might be small they cannot be disregarded out of hand since even a slight change in cathode field, brought about by a slight change in the space charge distribution, can produce significant changes in the emission current density. The treatment here includes the emission velocity spectrum predicted by quantum mechanics and the analysis is carried out in terms of parameters that enable the results to be applied to any cathode material, anode voltage and electrode separation. A plane parallel electrode geometry is chosen purely to enable the two successive integrations of Poisson's equation to be carried out exactly in analytic form.

2. First integration of Poisson's equation

The formulation of the general space charge problem follows closely the treatment given by Fry (1921) in his study of thermal emission and recently applied by Wheeler (1972) to photoelectric emission. In the case of these emission processes, space charge can produce a potential minimum between the electrodes and the associated reversed field repels some electrons back to the cathode. The net result is that the anode current can be very much less than the primary emission current. However, for the case of field emission, the potential distribution must increase monotonically from cathode to anode and the effect of space charge is to reduce the field in the cathode region, not to reverse it. The anode current is therefore always equal to the primary emission current. Absence of a potential minimum simplifies the problem since the inter-electrode region can mathematically be regarded as one region of space.

Consider a plane parallel electrode configuration, situated in vacuum, and let the cathode emit a steady stream of electrons with normal velocity component u such that $n(u)\,\mathrm{d}u$ is the number of electrons emitted per unit area and time with normal velocities in the interval u, $\mathrm{d}u$. The emission current density is therefore

$$J = e\int_0^\infty n(u)\,\mathrm{d}u. \tag{1}$$

Let x denote the position and V the potential of a point in the electron cloud, both measured relative to the cathode surface. If all potentials are such that the treatment can be nonrelativistic then the electron velocity v at the point x is given by

$$\tfrac{1}{2}mv^2 = \tfrac{1}{2}mu^2 + eV. \tag{2}$$

The space charge density at any point is obtained by dividing the number of electrons passing through unit area per unit time by their local velocity:

$$\rho = -e\int_0^\infty \frac{n(u)}{v}\,\mathrm{d}u. \tag{3}$$

This space charge must be related to the potential V through Poisson's equation:

$$\frac{\mathrm{d}^2V}{\mathrm{d}x^2} = -4\pi\rho = 4\pi e\int_0^\infty \frac{n(u)}{v}\,\mathrm{d}u.$$

Multiply both sides of this equation by $2dV/dx$ where, from equation (2), $dV/dx = (mv/e)\,dv/dx$. This factor can go inside the integration since dV/dx is not a function of u. Poisson's equation then becomes

$$\frac{d}{dx}\left(\frac{dV}{dx}\right)^2 = 8\pi m \int_0^\infty n(u)\,du\,\frac{dv}{dx}.$$

Now integrate both sides of this equation with respect to x, remembering that u is not a function of x:

$$\left(\frac{dV}{dx}\right)^2 - E_0^2 = 8\pi m \int_0^\infty (v-u)n(u)\,du, \tag{4}$$

where $E_0 = -(dV/dx)_0$ is the electric field at the cathode surface. E_0 and $n(u)$ must now be related by field emission theory and the integration over electron velocity performed before the second integration with respect to x can be carried out.

3. Electron emission velocity spectrum

Application of a large positive potential gradient to the surface of a metal distorts the shape of the potential barrier confining the electrons within the metal. Relative to the top of the unperturbed barrier the potential describing the force on an isolated electron situated in vacuum just in front of the conducting cathode surface, in the presence of an applied field E_0, can be expressed,

$$V_0(x) = -eE_0x - \frac{e^2}{4x} \qquad x > 0. \tag{5}$$

Figure 1 shows the form of this potential. Let $n(W)\,dW$ be the number of electrons per unit area and time that penetrate the barrier with *incident* energies, normal to the metal surface, in the interval W, dW. This number is equal to the number that strike the barrier per unit area and time, obtained from Fermi–Dirac statistics, multiplied by the

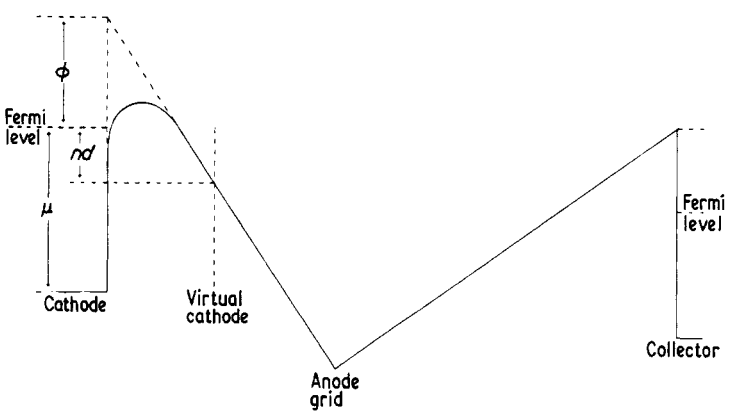

Figure 1. Schematic representation of cathode potential barrier and electrode configuration in a retarding field experiment.

barrier transmission. Fowler and Nordheim (1928) calculated this transmission for a ramp barrier, that is, for the E_0 term in equation (5), and Nordheim (1928) extended the treatment to include the remaining image term. At temperatures sufficiently low for there to be a negligible population above the Fermi level in the cathode metal the result assumes the following simple form:

$$n(W)\,\mathrm{d}W = \frac{4\pi m}{h^3}\exp(-c)(\mu - W)\exp\left(-\frac{(\mu - W)}{d}\right)\mathrm{d}W, \qquad 0 \leqslant W \leqslant \mu, \tag{6}$$

where μ is the potential of the Fermi level relative to the bottom of the potential well, as indicated in figure 1, and

$$\begin{aligned} c &= \frac{8\pi}{3heE_0}(2m\phi^3)^{\frac{1}{2}}A, \\ d &= \left(\frac{8\pi}{heE_0}\right)^{-1}(2m\phi)^{-\frac{1}{2}}B^{-1}. \end{aligned} \tag{7}$$

ϕ is here the cathode work function, A and B are functions of the parameter e^3E_0/ϕ^2, tabulated by Burgess *et al* (1953). The parameter d is a convenient quantity for defining an energy scale since the spectrum $n(W)$ of equation (6) has its maximum at $W = \mu - d$, that is, at an energy d below the Fermi level. The total emission current of equation (1) is also the integral of $n(W)$ over all possible incident energies, that is $0 \leqslant W \leqslant \mu$. If $y = (\mu - W)/d$, then the total current density is

$$\begin{aligned} J &= \frac{4\pi emd^2}{h^3}\exp(-c)\int_0^{\mu/d} y\exp(-y)\,\mathrm{d}y \\ &= \frac{4\pi emd^2}{h^3}\exp(-c)\left\{1-\left(1+\frac{\mu}{d}\right)\exp\left(-\frac{\mu}{d}\right)\right\}. \end{aligned} \tag{8}$$

For all practical values of E_0 the parameter $\mu/d \gg 1$, consequently, to a very good approximation,

$$J = \frac{4\pi emd^2}{h^3}\exp(-c). \tag{9}$$

Equations (7) and (9) constitute the FN equation for field emission current. The exponential term is the dominant factor and if lg J is plotted against $1/E_0$ a near straight line is obtained as shown, for example, in figure 4.

The electron emission velocity spectrum follows directly from equation (6) but the electrons cannot be represented classically outside the metal surface, until they have penetrated through the potential barrier. Since the thickness of the barrier is a function of the incident energy W, as shown in figure 1, there is some uncertainty in the mathematical representation of the cathode surface. Consider a plane virtual cathode parallel to the physical cathode and positioned a certain distance in front of it such that the bulk of the emission current has penetrated the barrier at this position. Let this cathode be at an energy nd below the Fermi level, as indicated in figure 1, where n is a pure number. Then, following equation (8), the emission current that has penetrated the barrier at this virtual cathode position is,

$$J(n) = \frac{4\pi emd^2}{h^3}\exp(-c)\{1-(1+n)\exp(-n)\}. \tag{10}$$

The electrons with incident energy $W < nd$ that constitute the current $J-J(n)$ are still inside the barrier at this position and cannot be treated classically. Relative to this virtual cathode the emission velocity u is,

$$\tfrac{1}{2}mu^2 = W-(\mu-nd), \qquad 0 \leqslant W \leqslant \mu. \tag{11}$$

Before considering the choice of value for n it should be noted that the emission spectrum $n(u)$, defined by equations (6) and (11), is in complete agreement with the measurements made by Henderson and Dahlstrom (1939). Their apparatus, represented schematically by the whole of figure 1, consisted of a tungsten cathode, an accelerating anode grid through which the electrons could pass and enter a much weaker but more extensive retarding field region, and finally a collector electrode. The integrated electron velocity spectrum was examined by varying the potential of the collector relative to that of the cathode. It was found that the collector potential had to be made positive with respect to the cathode by an amount equal to at least the work function of the collector material before any electrons were collected. Referring to figure 1 this meant that the surface of the collector, which had a relatively thick potential barrier, had to be at the same potential as the Fermi level of the cathode. Now suppose that the virtual cathode is placed at this position, that is $n = 0$, then equation (11) indicates that the maximum emission energy of the electrons is zero. Consequently, in order that these electrons should pass over the broad barrier at the collector surface, it is necessary that this surface be raised to at least the same potential as the cathode Fermi level, which was the situation required experimentally. By further increasing the collector potential Henderson and Dahlstrom (1939) were able to infer the complete emission spectrum and found good agreement with equation (6) except in the low energy tail where secondary emission in their apparatus prevented close investigation.

Substitution of equations (11) and (6) into equation (4) and performing the integrations over velocity, with V and x now measured relative to the virtual cathode, results in,

$$\begin{aligned}\left(\frac{\mathrm{d}V}{\mathrm{d}x}\right)^2 - E_0^2 = \frac{32\pi^2m^2d^2}{h^3}\left(\frac{2d}{m}\right)^{\frac{1}{2}}\exp(-c) \\ \times\left[\frac{3}{2}\left(n+\frac{eV}{d}\right)^{\frac{1}{2}} - \left(n+\frac{3}{2}+\frac{eV}{d}\right)D\left\{\left(n+\frac{eV}{d}\right)^{\frac{1}{2}}\right\} - \frac{3}{2}n^{\frac{1}{2}}\right. \\ + \left(n+\frac{3}{2}\right)D\{n^{\frac{1}{2}}\} + \exp(-n)\left\{\left(n+\frac{3}{2}+\frac{eV}{d}\right)D\left\{\left(\frac{eV}{d}\right)^{\frac{1}{2}}\right\}\right. \\ \left.\left. - \left(n+\frac{3}{2}\right)\left(\frac{eV}{d}\right)^{\frac{1}{2}}\right\}\right],\end{aligned} \tag{12}$$

where $D\{x\} = \exp(-x^2)\int_0^x \exp(t^2)\,\mathrm{d}t$ is Dawson's integral. This integral approaches zero as $x \to 0$ or $x \to \infty$, and, in the latter case, has the asymptotic form $D\{x\} \to 1/2x$.

A suitable value for the parameter n can be inferred from equation (10) which gives the fraction $J(n)/J$ of the total current that can be regarded as a free electron gas at the virtual cathode. For example $n = 7$, giving $J(7)/J = 0{\cdot}993$, allows classical treatment of the bulk of the emitted electrons. Such a value of n will underestimate space charge effects since the peak of the emission spectrum, occurring at $W = \mu-d$, will have an associated emission energy $\frac{1}{2}mu^2 = 6d$ and, from equation (3), the greater the velocity the smaller the space charge. On the other hand an overestimate of space charge effects can be obtained by assuming that all electrons have zero emission velocity. In

this case the emission spectrum $n(u)$ must be regarded as a delta function at $u = 0$ in order that the total current can be defined by equation (1). Equations (1), (2) and (4) then give directly,

$$\left(\frac{dV}{dx}\right)^2 - E_0^2 = \frac{8\pi mJ}{e}\left(\frac{2e}{m}\right)^{\frac{1}{2}} V^{\frac{1}{2}}. \tag{13}$$

4. Second integration of Poisson's equation

If the parameter n in equation (12) is sufficiently large then a great simplification can be brought about by neglecting the terms multiplied by the exponential and by replacing the Dawson integral by its asymptotic expression. These operations give,

$$\left(\frac{dV}{dx}\right)^2 - E_0^2 = \frac{32\pi^2 m^2 d^2}{h^3}\left(\frac{2d}{m}\right)^{\frac{1}{2}} \exp(-c)\left\{\left(n+\frac{eV}{d}\right)^{\frac{1}{2}} - n^{\frac{1}{2}} - \delta\left(n, \frac{eV}{d}\right)\right\} \tag{14}$$

where δ is a correction that approaches zero as $V \to 0$ or as $V \to \infty$. For $n = 7$ this correction is most significant in the region $0 < eV < 7d$ where it amounts to 3·3 % of the remaining terms. Further simplification results if this correction is neglected and if the following new variables are introduced:

$$X = \frac{128\pi^2 mJ^2}{e}\frac{x}{E_0^3}, \qquad Y = \frac{128\pi^2 mJ^2}{e}\frac{V}{E_0^4}, \qquad Z = \frac{128\pi^2 mJ^2}{e}\frac{d}{e}\frac{n}{E_0^4}. \tag{15}$$

With these substitutions and use of equation (9), equation (15) takes the simple form:

$$\left(\frac{dY}{dX}\right)^2 = (Y+Z)^{\frac{1}{2}} - Z^{\frac{1}{2}} + 1, \tag{16}$$

which can be integrated directly to give,

$$X = \tfrac{4}{3}[\{1+(Y+Z)^{\frac{1}{2}} - Z^{\frac{1}{2}}\}^{\frac{3}{2}} - 3(1-Z^{\frac{1}{2}})\{1+(Y+Z)^{\frac{1}{2}} - Z^{\frac{1}{2}}\}^{\frac{1}{2}} - 3Z^{\frac{1}{2}} + 2]. \tag{17}$$

This equation inherently contains the more simplified treatments of previous workers. For example, putting $Z = 0$ and neglecting unity in equation (16), which is equivalent to putting $E_0 = 0$ in equation (13), leads to,

$$X = \tfrac{4}{3}Y^{\frac{3}{2}}$$

or

$$J_{LC} = \frac{1}{9\pi}\left(\frac{2e}{m}\right)^{\frac{1}{2}}\frac{V^{\frac{3}{2}}}{x^2}. \tag{18}$$

This is the Langmuir (1913) and Child (1911) (LC) equation for fully space charge limited emission; it is valid for any emission process under the assumptions of zero field and velocity at the cathode surface. If, on the other hand, $Z = 0$ but unity is retained, then equations (16) and (13) are the same and represent the general case of overestimation of space charge effects considered by Barbour *et al* (1953). Consequently the exact form of the potential distribution between the electrodes must be somewhere between the expressions given by equation (17) for $Z = 0$ and $Z(7)$ which correspond, respectively, to an overestimate and an underestimate ($n = 7$) of space charge effects.

For the case of pure field emission considered here there is an upper limit to $Z(7)$ imposed by the condition that the potential barrier at the cathode should always be

greater in energy than the highest level occupied by the electrons within the metal. On account of the image term in equation (5) the barrier is reduced in height (Schottky effect), as well as in width, as E_0 is increased. Differentiation with respect to x shows that the maximum of the barrier lies above the Fermi level provided $E_0 < \phi^2/e$. If this condition is not satisfied then electron emission by 'thermal evaporation' over the top of the barrier can take place, even at zero temperature, and the foregoing analysis would be inaccurate. The function A in equation (7) approaches zero as this limiting cathode field is approached and equations (7), (9) and (15) then define the following upper limits to J and $Z(7)$ for which the emission is purely by barrier penetration at zero temperature:

$$E_0 < 6{\cdot}94 \times 10^6\, \phi^2 \text{ V cm}^{-1}, \qquad J < 7{\cdot}41 \times 10^7\, \phi^3 \text{ A cm}^{-2}, \qquad Z(7) < 0{\cdot}655\, \phi^{-\frac{1}{2}}, \tag{19}$$

where ϕ is expressed in electron volts. In particular $Z(7)$ is less than unity for all cathode materials.

Figure 2 shows a logarithmic plot of equation (17) for the two extremes $Z = 0$ and $Z = 1$. The axes here scale with J and E_0 according to equation (15) and J is the dominant factor. Small values of X and Y correspond to the passage of small currents and in this region the curves approximate to $X = Y$. This is simply the uniform field relation $V = E_0 x$ which is physically expected at low currents when space charge effects are negligible. For larger values of X and Y the $Z = 0$ curve is the first to deviate from the $X = Y$ relation since this curve represents an overestimate of space charge effects. At the other extreme, for sufficiently large values of J, the potential distribution in the anode region approaches the LC equation (18), $X = \frac{4}{3}Y^{\frac{3}{4}}$.

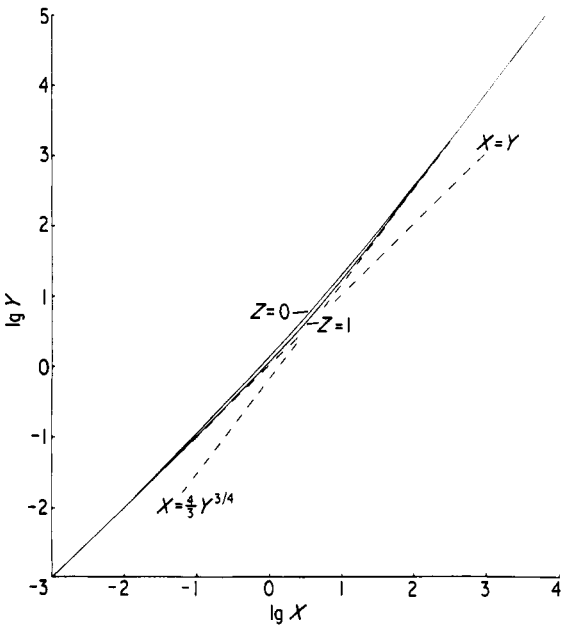

Figure 2. Inter-electrode potential distribution according to equation (17) for the two extremes $Z = 0$ and $Z = 1$.

5. Application of the results

In most applications of field emission it is the current density J that is required as a function of the applied anode voltage V_A for given values of the electrode spacing x_A and specified cathode work function ϕ. In principle the (J, V_A) characteristic can be determined from figure 2 in conjunction with the FN equation for the relevant cathode but the technique is iterative and laborious. A much simpler technique is to construct an intermediate graph of X/Y against $\lg X$ with X and Y evaluated at the anode, that is, at $x = x_A$ and $V = V_A$. In this case it follows from equation (15) that,

$$\frac{X}{Y} = \frac{E_0 x_A}{V_A} = \frac{E_0}{\bar{E}},$$

where $\bar{E} = V_A/x_A$ is the field in the absence of space charge effects. Figure 3 shows the results of the computations for $Z = 0$, 0·01 and 0·10. The abscissa is presented

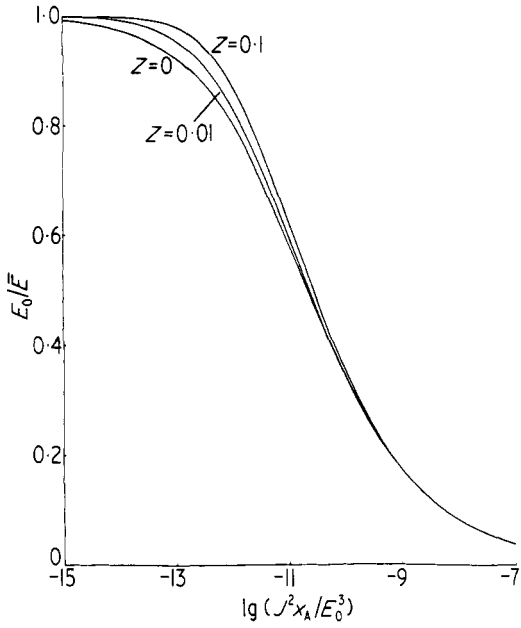

Figure 3. Cathode field reduction $E_0/\bar{E}$ produced by space charge, as a function of current density J (A cm^{-2}), electrode spacing x_A (cm) and cathode field E_0 (V cm^{-1}) for three values of the parameter Z.

numerically with J expressed in A cm^{-2}, E_0 in V cm^{-1} and x_A in cm. In these same units and with ϕ in electron volts,

$$Z(7) = 3{\cdot}98 \times 10^4 \, \phi^{-\frac{1}{2}} \frac{J^2}{E_0^3}. \tag{20}$$

Physically figure 3 presents the fractional reduction in field at the cathode surface, caused by space charge, as a function of emission current and electrode spacing. This figure must be used along with calculations based on the FN equation such as those

shown in figure 4 for tungsten. The numerical computations of Dolan (1953) were used for this figure and the parameter J^2/E_0^3 also computed to enable X and $Z(7)$ to be evaluated. Figures 3 and 4 were used together to compile figure 5 for tungsten in the following manner. Firstly a value of E_0 was selected and J and J^2/E_0^3 determined from figure 4. For a given x_A this enables $E_0/\bar{E}$ to be evaluated from figure 3 for both $Z = 0$ and $Z(7)$. Consequently the anode potential, $V_A = x_A E_0(\bar{E}/E_0)$, required to produce the current J was determined. By selecting a range of initial values of E_0 it was possible

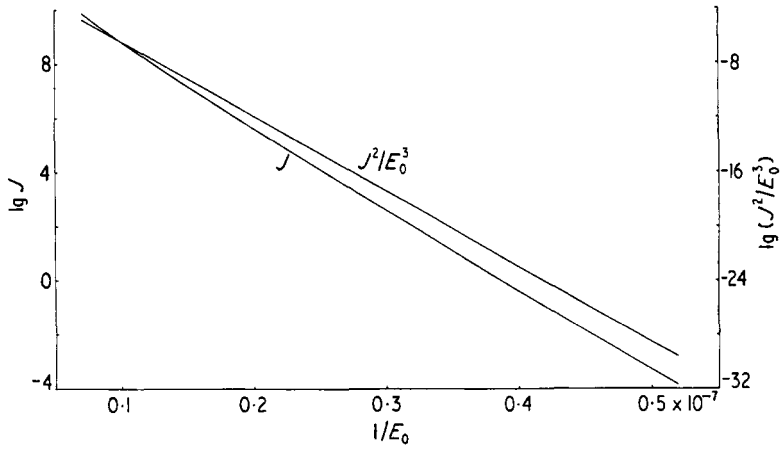

Figure 4. Current density J (A cm^{-2}) and J^2/E_0^3 for tungsten as a function of cathode field E_0 (V cm^{-1}) according to FN theory.

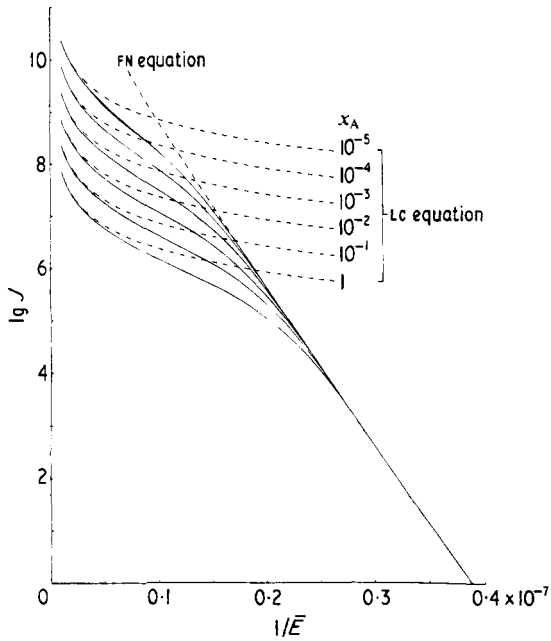

Figure 5. Current density J (A cm^{-2}) as a function of applied field $\bar{E}$ (V cm^{-1}) and electrode spacing x_A (cm) for tungsten.

to evaluate the (J, V_A) characteristic for given values of x_A. The axes J and $1/\bar{E}$ were chosen for figure 5 in order to show the departure from the FN equation at large values of J and the subsequent approach to the LC equation as space charge effects became dominant. A wide range of x_A was used (1 cm to 10^{-5} cm) in order to embrace both the experimental plane parallel geometries and also the more usual near hyperboloidal, conical and hemispherical cathode shapes. For these latter cases (Dyke and Trolan 1953, Dyke *et al* 1953, Barbour *et al* 1953) it is customary to apply plane parallel emission theory simply by defining an effective x_A that gives the same space charge free cathode field $\bar{E}$ in parallel geometry as that calculated for the relevant experimental geometry, both for the same applied V_A. It must be emphasized that this technique is acceptable when space charge effects are negligible and a good approximation in the region where departure from the FN equation begins. However the technique will not be valid when space charge effects become dominant since the numerical factor in the LC equation (18) is a function of the electrode geometry. The references cited here quote values of x_A down to 5×10^{-5} cm. It is only for such small values of x_A that the LC limiting current is greater than the current required to make $Z(7)$ for tungsten significantly different from zero. This is shown in figure 5 for $x_A = 10^{-5}$ cm where the two curves, representing upper and lower limits to space charge effects, just separate before complete limitation takes place.

6. Discussion

The departure of the measured currents from the FN equation, shown in figure 5 for tungsten, can be expressed quantitatively as follows. From figure 3, $E_0/\bar{E} = 0{\cdot}90$ when $J^2 x_A/\bar{E}^3 = 1{\cdot}36 \times 10^{-13}\,\mathrm{A^2\,V^{-3}}$, or, using equation (18), when $J = 0{\cdot}16\,J_{LC}$ where J_{LC} is evaluated at the relevant x_A and V_A. Consequently when the emission current, as calculated from the FN equation, reaches 16 % of the LC limiting current, the slope of the lg J against $1/\bar{E}$ plot will have deviated by 10 % from that given by the FN equation.

Although the effects of finite velocity of emission are too small to be significant in the case of tungsten, the effect becomes more pronounced for cathodes of lower work function. Figure 3 indicates that differing values of Z are only significant in the region where space charge is mildly affecting the cathode field. For example the ordinates for the curves $Z = 0$ and $Z = 0{\cdot}01$ have a maximum separation of 3·8 % in the region $E_0/\bar{E} = 0{\cdot}9$. If the value $Z(7) = 0{\cdot}01$ is taken as the criterion for the onset of significant emission velocity effects, then equations (7), (9) and (20) can be solved for the value of J, as a function of ϕ, at which this onset occurs and figure 6 shows the results of such calculations. For tungsten ($\phi = 4{\cdot}5$ eV) the onset occurs at the high value of lg $J = 8{\cdot}9$ but for cathodes of lower work function the current for onset is within the range that can be attained experimentally. However it must be emphasized that emission velocity effects only occur if the experimental parameters V_A and x_A are such that this value of J lies somewhere in the transition region between the FN equation and the LC equation, that is, for roughly $0{\cdot}2 < J/J_{LC} < 0{\cdot}8$.

In the past few years field emission has been widely used to produce very high currents for electron beam experiments. The FN equation shows that V_A and x_A should be chosen to make $\bar{E}$ as large as possible in order that the strong dependence of J on E_0 can be employed. However the foregoing discussion shows that J_{LC} must also be sufficiently large if the benefits of the FN equation are not to be destroyed by the presence of space charge. If the previous relation, $J = 0{\cdot}16\,J_{LC}$, is taken as the criterion for

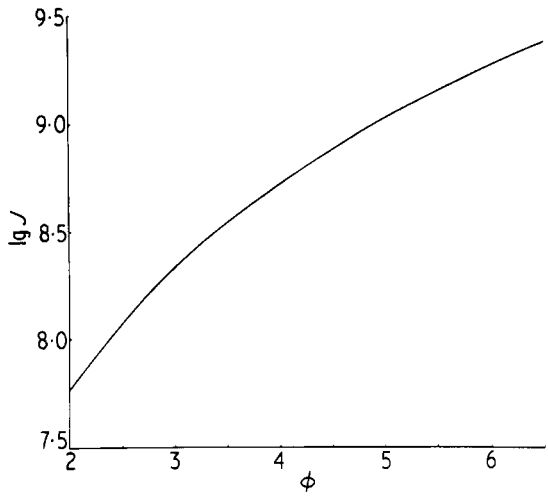

Figure 6. Current density J (A cm^{-2}), above which emission velocity effects are important, as a function of cathode work function ϕ (eV).

departure from the FN equation then equations (7), (9) and (18) can be solved for the value of V_A at which departure takes place as a function of x_A and ϕ. It is more useful to express the results in the form of an $\bar{E}$ against lg x_A graph, as shown in figure 7, as this enables application to other geometries. The work functions displayed here include tungsten and platinum and the FN computations of Dolan (1953) were used for the calculations. It must be noted that, in the case of platinum, the magnitude of the work function is very dependent on the technique of measurement, the degree of out-gassing

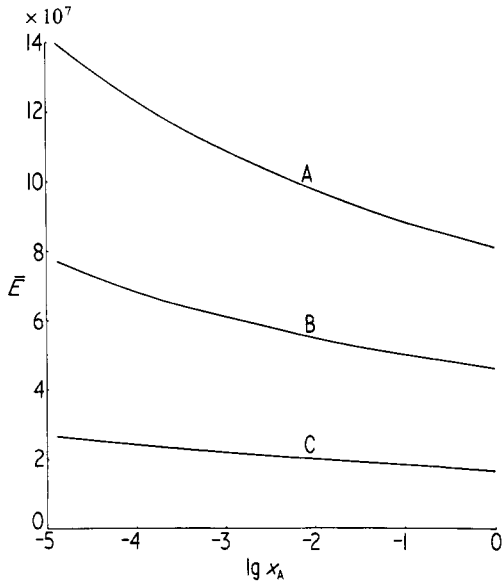

Figure 7. Applied field $\bar{E}$ (V cm^{-1}), above which the FN equation is invalid, as a function of electrode spacing x_A (cm) and cathode work function ϕ (eV). Curve A, platinum, ϕ = 6·3 eV; curve B, tungsten, ϕ = 4·5 eV; curve C, ϕ = 2·5 eV.

and the crystalline structure of the sample investigated. The recent table compiled by Weast (1972) quotes values between 4·52 and 6·35 eV with a preferred value of 5·32 eV which is considerably lower than the value of 6·3 eV assumed by Dolan and used in figure 7. If the experimental value of $\bar{E}$ lies on or above the curve for the relevant ϕ and x_A then considerably greater currents can be obtained, for the same $\bar{E}$, by reducing the value of x_A.

Finally it must be pointed out that the analysis here is nonrelativistic, assumes that the cathode temperature is sufficiently low for there to be a negligible electron population above the Fermi level, and also assumes that emission is by barrier penetration, that is, the peak of the cathode potential barrier always lies above the Fermi level.

References

Barbour J P, Dolan W W, Trolan J K, Martin E E and Dyke W P 1953 *Phys. Rev.* **92** 45–51
Burgess R E, Kroemer H and Houston J M 1953 *Phys. Rev.* **90** 515
Child C D 1911 *Phys. Rev.* **32** 492–511
Cutler P H and Nagy D 1964 *Surface Sci.* **3** 71–94
Dolan W W 1953 *Phys. Rev.* **91** 510–1
Dyke W P and Trolan J K 1953 *Phys. Rev.* **89** 799–808
Dyke W P, Trolan J K, Dolan W W and Barnes G 1953 *J. appl. Phys.* **24** 570–6
Fowler R H and Nordheim L W 1928 *Proc. R. Soc.* A **119** 173–81
Fry T C 1921 *Phys. Rev.* **17** 441–52
Henderson J E and Dahlstrom R K 1939 *Phys. Rev.* **55** 473–81
Langmuir I 1913 *Phys. Rev.* **2** 450–86
Nordheim L W 1928 *Proc. R. Soc.* A **121** 626–39
Norwicki R 1967 *Surface Sci.* **8** 357–69
Stern T E, Gossling B S and Fowler R H 1929 *Proc. R. Soc.* A **124** 699–723
Weast R C 1972 *Handbook of Chemistry and Physics* (Cleveland, Ohio: Chemical Rubber Co.) p E-70
Wheeler C B 1972 *J. Phys.* A: *Gen. Phys.* **5** 1337–54